

Journal of Materials Chemistry A

Accepted Manuscript



This is an *Accepted Manuscript*, which has been through the Royal Society of Chemistry peer review process and has been accepted for publication.

Accepted Manuscripts are published online shortly after acceptance, before technical editing, formatting and proof reading. Using this free service, authors can make their results available to the community, in citable form, before we publish the edited article. We will replace this *Accepted Manuscript* with the edited and formatted *Advance Article* as soon as it is available.

You can find more information about *Accepted Manuscripts* in the [Information for Authors](#).

Please note that technical editing may introduce minor changes to the text and/or graphics, which may alter content. The journal's standard [Terms & Conditions](#) and the [Ethical guidelines](#) still apply. In no event shall the Royal Society of Chemistry be held responsible for any errors or omissions in this *Accepted Manuscript* or any consequences arising from the use of any information it contains.

Graphic Abstract for
Colorimetric Strips for Visual Lead Ion Recognition Utilizing
Polydiacetylenes Embedded Nanofibers

Yan Li^a, Lihuan Wang^a, Xia Yin^a, Bin Ding^{a, b}, Gang Sun^b, Tao Ke^c,
Jingyuan Chen^{c*}, and Jianyong Yu^a*

^a Key Laboratory of Textile Science & Technology, Ministry of Education, College of Textiles, Donghua University, Shanghai 201620, China

^b Nanomaterials Research Center, Modern Textile Institute, Donghua University, Shanghai 200051, China

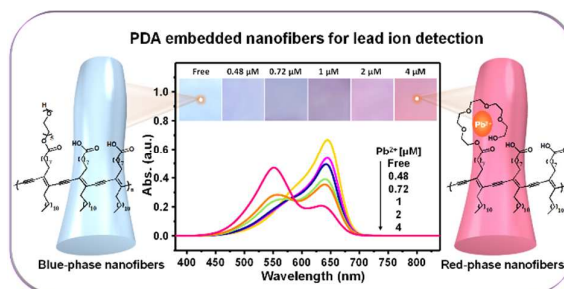
^c Department of Occupational and Environmental Health, School of Public Health, Fourth Military Medical University, Xi'an, Shanxi 710032, China

* Corresponding author at: Key Laboratory of Textile Science & Technology, Ministry of Education, College of Textiles, Donghua University, Shanghai 201620, China.

Fax: +86 21 62378392.

E-mail: binding@dhu.edu.cn (B. Ding) and jy_chen@fmmu.edu.cn (J. Chen)

Graphic Abstract



A portable, sensitive and selective colorimetric strip for naked-eye recognizing of Pb²⁺ utilizing solid-phase polydiacetylenes embedded electrospun polyacrylonitrile nanofibers

ARTICLE

Colorimetric Strips for Visual Lead Ion Recognition Utilizing Polydiacetylenes Embedded Nanofibers

Cite this: DOI: 10.1039/x0xx00000x

Yan Li,^a Lihuan Wang,^a Xia Yin,^a Bin Ding,^{a, b*} Gang Sun,^b Tao Ke,^c Jingyuan Chen,^{c*} and Jianyong Yu^b

Received 00th January 2012,

Accepted 00th January 2012

DOI: 10.1039/x0xx00000x

www.rsc.org/

Given the dire consequences of accidental lead ion (Pb^{2+}) exposure, a portable, sensitive and robust analytical approach capable of colorimetric visualization is highly desirable. In this study, we demonstrate a colorimetric strip that relies on a novel polydiacetylene (PDA) embedded polyacrylonitrile nanofibrous membranes (PAN NFM). The Pb^{2+} -chromic PDA is prepared from controlled mixtures of 10, 12-Pentacosadiynoic acid (PCDA) and PCDA-5EG, a PCDA derivative with a pentaethylene glycol headgroup. Moreover, the Pb^{2+} complexation ability is manipulated by controlling the molar ratio of PCDA to PCDA-5EG. PAN NFM acting as a three dimensional matrix is designed for PDA immobilization, thereby improving the stability, portability and sensitivity. Upon exposure to a series of metal ions, only Pb^{2+} could induce a color change, which clearly showed that our strip could act as a highly selective probe to detect Pb^{2+} . Ultimately, the strip with a naked eye detection limit of $0.48 \mu\text{M}$ undergo a brilliant color transition, from blue-to-red, in a concentration-dependent manner and all the color transitions of strips are quantitatively visualized by employing a chromatic framework. The findings indicate that strip is particularly promising for visual Pb^{2+} recognition due to its facile functionalization, simple construction, and the versatility to empower colorimetric signaling.

Introduction

Non-biodegradable lead has historically been, and remains today, a persistent contaminant in the environment. It has been found that a trace amount of lead in blood could result in decreased intelligence and impaired neurobehavioral development.¹⁻³ Accordingly, the Centers for Disease Control and Prevention has strictly defined that the whole blood lead concentration $> 0.48 \mu\text{M}$ in children as indicative of significant exposure and recommends chelation therapy.^{4, 5} Given the environmental availability of Pb^{2+} and the dire consequences of accidental exposure, especially to children, it is not surprising that people are pushing hard to develop sensitive and robust analytical approaches for sensing of Pb^{2+} in the field.

The most commonly used techniques for laboratory scale Pb^{2+} determinations have been atomic absorption spectroscopy⁶ and inductive coupled plasma emission spectrometer,⁷ due mainly to their high accuracy. However, the sophisticated equipment, high cost or tedious sample treatment have compromised their practicability in simple, portable, and point-of-care discrimination of Pb^{2+} .⁸⁻¹⁰ In parallel to the development of sophisticated equipment, variety of detection schemes,

including colorimetric,^{9, 11} fluorescent,¹² and electrochemical¹³ approaches have been widely studied. Among them, colorimetric readout is a desirable sensing technique as it is highly useful to field technicians and emergency responders, owing to the portability and relatively low cost of the devices.^{14, 15} Until now, considerable efforts have been devoted to the Pb^{2+} detection utilizing different receptors like DNazymes,¹⁶ peptides,¹⁷ and dyes.¹⁸ However, sensors based on those macromolecules are still lack portability, relatively unstable, and even some of them have no selectivity. Thus the development of portable, selective, and sensitive colorimetric Pb^{2+} sensors is still a challenging problem.

As a family of colorimetric receptors, π -conjugated polymers, polydiacetylenes (PDA) exhibit a blue-to-red phase transition characteristic that can be triggered when external stimuli, including heat (thermochromism),¹⁹⁻²¹ mechanical stress (mechanochromism),^{22, 23} and ligand-receptor interactions (affinochromism),²⁴⁻²⁷ etc. distort the conjugated π -ene main chain. Importantly, through a rational monomers design, the PDA could be adopted in the development of various sensors for specific target molecules.^{28, 29} Such characters are of a great

merit to make them attractive in sensing area. However, only a few papers describing the PDA based Pb^{2+} sensors have been reported, and all of them are in liposome form.^{30,31} It should be noted that the liposomes have a few limitations: long-term storage is difficult because of intrinsic aggregation,^{32, 33} uncertainty with respect to concentration, and the low sensitivity due to homogenous dilution of liposome and targets in solutions.^{34, 35}

On the other hand, immobilization of PDA on a solid substrate or fibers have been actively investigated.³⁶ The last decade has witness diverse examples include microarrays,^{25, 29, 37} thin films,³⁸ electrospun nanofibers,^{39, 40} and microbeads.⁴¹ Amongst them, electrospun nanofibers have gained much attention owing to their inherently high specific surface area (SSA), small interfibrous pore size, and good interconnectivity.⁴²⁻⁴⁵ In this regard, Davis *et al.* demonstrated that PDA embedded into nanofibers could be used as a colorimetric sensors for organic vapors exhibits an enhanced stability.^{34, 46} Nanofibers thus has become an attractive candidate as matrix for PDA immobilization.

In this contribution, we have uncovered a very intriguing approach to colorimetric quantitative detection of Pb^{2+} . As illustrated in Scheme 1, a strip has been fabricated by embedding a new synthesized PDA into the electrospun polyacrylonitrile nanofibrous membranes (PAN NFM). The PDA composed of 10, 12-Pentacosadiynoic acid (PCDA) and PCDA-5EG, a PCDA derivative with a pentaethylene glycol (5EG) headgroup is responsible for Pb^{2+} complexation and signal generation.^{47, 48} Although Narkwiboonwong *et al.*⁴⁹ have demonstrated that PDA liposome containing oligoethylene oxide headgroups could be used as a colorimetric sensor for Pb^{2+} , the aforementioned inherent limitation of liposome have restricted its sensing performance. Herein, the PAN NFM acting as matrix for PDA immobilization would endow the strip enhanced portability, stability and increased SSA, so that the strip shows better sensitivity.^{40, 41, 49} To our best knowledge, there has been no reported work on using PDA for detection of Pb^{2+} with this solid support and no effort has been made to differentiate the color change of PDA system utilizing a quantitative method. This work may offer a new avenue for developing robust colorimetric strip that meet the needs of portable, easy-to-use, sensitive, and selective visual Pb^{2+} recognition.

Experiments

Materials and reagents

The diacetylene monomers (DAs), PCDA, and *N*-(2-hydroxyethyl) piperazinyl-*N*-2-ethanesulfonic acid buffer (HEPES, 1 mM, pH 7.4) were provided by Aladdin Co., Ltd., China. 5EG was applied by Shuya Shanghai Co., Ltd. Toluene, methylene chloride, sulfuric acid, Na_2CO_3 , MgSO_4 , and *N,N*-dimethylformamide (DMF) were provided by Shanghai Chemical Reagents Co., Ltd. PAN ($M_n = 90\ 000$) was obtained from Spectrum Chemicals & Laboratory Products Co. Ltd.

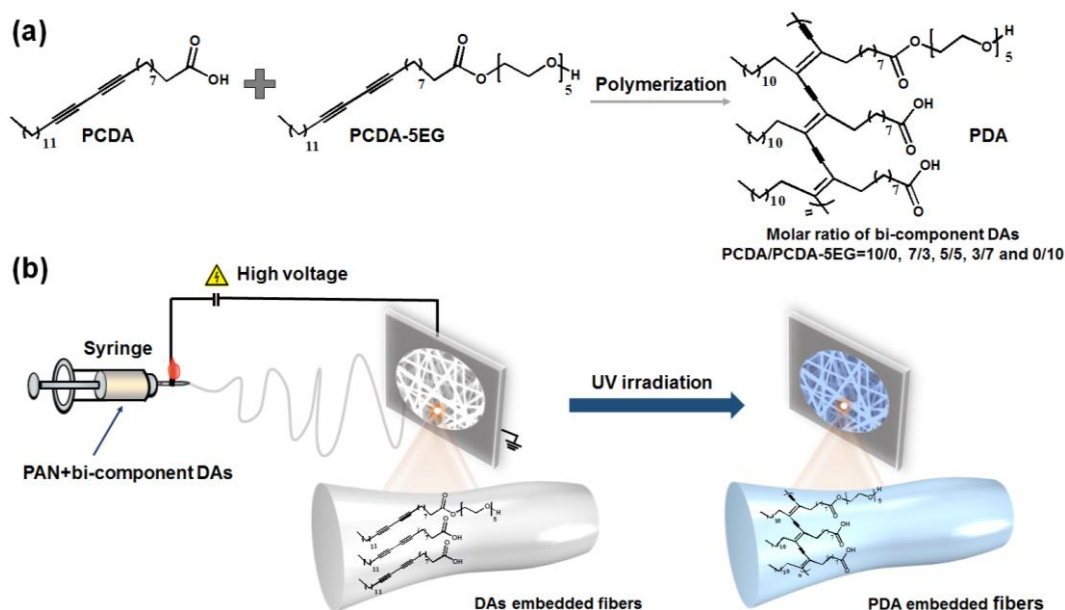
Nitrate salts (K^+ , Na^+ , Ca^{2+} , Fe^{2+} , Fe^{3+} , Cu^{2+} , Cd^{2+} , Co^{2+} , Ni^{2+} , Cr^{3+} , Hg^{2+} , Zn^{2+} , and Pb^{2+}) used for all sensing experiments were supplied by Sigma-Aldrich Chemicals. Ultra-pure water with a resistance of 18.2 $\text{M}\Omega$ was prepared by a Heal-Force system. All chemicals were of analytical grade and used as received.

Synthesis the PCDA-5EG

Another new DAs, PCDA-5EG was synthesized *via* a four-step reaction. Typically, 312.8 mg PCDA was dissolved in 10 mL toluene in a 50 mL round bottom flask, and a 0.6 mL of 10.77 mmol ethylene glycol solution as well as 0.05 mL sulfuric acid were added to above solution with a magnetic stirrer. Then, the mixture was refluxed for 5 h at 100°C, allowed to cool to room temperature and the solvent was evaporated under reduced pressure. Subsequently, the residue was dissolved with 50 mL CH_2Cl_2 and washed two times with 50 mL saturated Na_2CO_3 solution. The organic phase was then collected and dried over anhydrous MgSO_4 and the solvent was removed under reduced pressure. Finally, the product was further purified by column chromatographic purification. The structural confirmation by ^1H and ^{13}C nuclear magnetic resonance (NMR) spectroscopy recorded on a Bruker Avance 400 is displayed in ESI, Fig. S1 and S2. ^1H NMR (400 MHz, CDCl_3): δ 0.88 (t, 3H), 1.23-1.61 (m, 32H), 2.1-2.33 (t, 6H), 3.1-3.73 (m, 18H), 4.22 (t, 2H) and ^{13}C NMR (100 MHz, CDCl_3): δ 14.022, 19.09, 19.103, 22.585, 28.26, 28.755, 28.962, 28.933, 29.238, 29.374, 29.503, 29.522, 29.537, 31.814, 45.822, 61.551, 63.232, 69.099, 70.438, 70.465, 70.504, 72.551, 76.743, 77.061, 77.379, 173.716.

Preparation of PDA embedded PAN NFM

A series of viscous DMF solutions containing bi-component DAs (PCDA and PCDA-5EG with different molar ratio: 10/0, 7/3, 5/5, 7/3, and 0/10) and PAN were prepared for electrospinning, the concentration of PAN in precursor solution were adjusted to 4, 6 and 8 wt%, and the solid weight ratio of DAs to PAN was fixed to 5 wt% in all samples. Above bi-component DAs-containing precursor solutions were pumped through a capillary connected with a metal syringe needle at a constant feed rate of 1.5 mL/h by using DXES-1 spinning equipment (Shanghai Oriental Flying Nanotechnology Co., Ltd., China). The electrospinning chamber was kept with a constant temperature (23°C) and relative humidity (42%). The application of a high voltage (25 kV) to the metal syringe needle enable the generation of nanofibers, which were collected on the surface of a grounded slick paper (distance from the tip to the collector: 15 cm). The white NFM comprising of PAN and DAs were stored in the dark. Photopolymerization of DAs embedded nanofibers was carried out by UV irradiation at 254 nm (1 m W cm^{-2}) for 5 minutes (2.5 min each side) at 25°C, then the PDA embedded nanofibers with blue color were obtained. The morphology of membranes was examined by using a field emission scanning electron microscopy (FE-SEM, S-4800, Hitachi Ltd., Japan). Apart from that, the Brunauer-Emmett-Teller (BET) surface area of membranes were characterized by using N_2 adsorption-



Scheme 1 (a) Self-assembly and polymerization of PCDA and PCDA-5EG. (b) Schematic representation of the preparation of PDA embedded PAN NFM.

desorption isotherms with a surface area analyzer (ASAP 2020, Micromeritics Co., USA).

Preparation of PDA embedded PAN film

DAs embedded PAN flat film was carried out by drop-casting process. A DMF mixture solution containing bi-component DAs vesicle (PCDA/PCDA-5EG = 7/3) and 6 wt% PAN was drop-cast onto a slide glass. After solvent evaporation, the slide glass was irradiated with 254 nm UV light for 30 min, to form PDA embedded PAN casting film. Then, the blue-colored film was peeled from the slide glass. The morphology of film was examined by above mentioned FE-SEM.

Colorimetric recognition of Pb^{2+}

For the typical sensing experiment of Pb^{2+} , each PDA embedded PAN NFM was cut into a 10 mm \times 10 mm square-shaped piece to get the strip. Colorimetric change of the strip was induced by applying 10 mL of Pb^{2+} liquor (HEPES buffer spiked with Pb^{2+} at concentration range from 0.48 to 4 μM) equilibrated at 20–60°C for 0–60 min. Control experiments were performed using 10 mL of HEPES buffer equilibrated under the same condition. After that, the strips were removed from the solution, washed with 5 mL ultra-pure water and dried at room temperature. The assaying procedure of casting film-based one was same as above.

The absorption intensities of the strips were measured by using IS-30-6-R integrating sphere (Ideaoptics Technology Ltd.) attached to the Ideaoptics PG 2000+ fiber optic spectrometer. A quantitative value of the blue-to-red color transition is given by the colorimetric response (CR%) value which is defined as $\text{CR}\% = \frac{PB_0 - PB_1}{PB_0} \times 100\%$. Where $PB = A_{\text{blue}} / (A_{\text{blue}} + A_{\text{red}})$. A is the absorbance at either the “blue” component in the UV-vis

spectrum (645 nm) or the “red” component (550 nm). PB_0 is the red/blue ratio of the free sample, while PB_1 is the value obtained for the sample subjected to Pb^{2+} perturbations. As to the color difference, the color of the sensor strip was estimated qualitatively by naked-eye as well as converting a diffused reflectance spectrum into the CIE 1976 *Lab* color space and calculating the chromatic aberration. The nature of blue-to-red chromic transition of strip was also probed by using a micro-Raman spectroscopy system (in Via-Reflex, Renishaw, Co.) at a laser excitation wavelength of 785 nm.

Result and Discussion

Effect of monomer composition on the detectability of Pb^{2+}

In the first phase of our investigation, we ask whether the change in headgroup of DAs, would affect the molecular assembly and response of resulting strip. To address this issue, we initially selected a series of bi-component DAs embedded 6 wt% PAN NFM derived strips and incubated them individually with 0.48 μM Pb^{2+} liquor for 30 min at room temperature (25°C). Based on spectroscopic data, the color change was quantified by the CR% value. As shown in the Fig. 1a, of various compositions probed, only the strip derived from pure PCDA-5EG doesn't show any color response upon the addition of the Pb^{2+} because the self-assemblies of pure PCDA-5EG could not meet the topological requirements for polymerization.⁴⁰ A visual manifestation is also evident from the Fig. S3, the color of pure PDA-5EG embedded strips maintain white after UV irradiation.

On the other hand, as to other three strips derived from mixed PCDA/PCDA-5EG monomers (3/7, 5/5, and 7/3), the

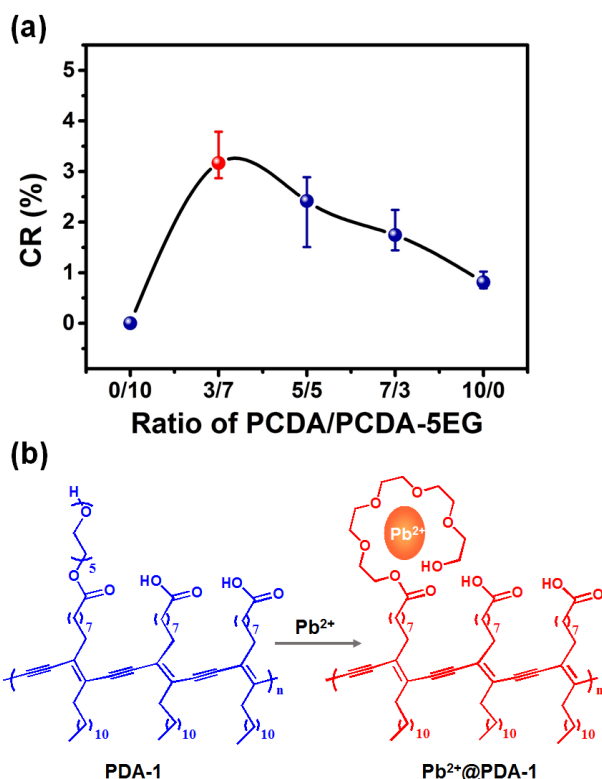


Fig. 1. (a) CR% values of strips derived from PCDA and PCDA-5EG with different mixing molar ratios (0/10, 3/7, 5/5, 7/3, and 10/0) towards to $0.48 \mu M Pb^{2+}$. (b) Proposed mechanism for the Pb^{2+} induced color transition.

CR% values increased gradually upon increasing the content of PCDA-5EG. Significantly, the strip derived from DAs in a mixing ratio of 3/7 showed the most dramatic color change of 3.1. Correspondingly, the PDA polymerized from molar ratio of 3/7 is denoted by PDA-1 and the strip is denoted as PDA-1/PAN-6 (where 6 is the concentration of PAN). In view of the color change results, we envision that the 5EG group plays a vital role for Pb^{2+} recognition. To substantiate this proposition, a pure PCDA derived strip was further investigated. Even though it is known that the carboxylic acid group in PCDA can coordinate to Pb^{2+} ,³⁰ there induces a color shift clearly discernable to the naked eye (CR% = 0.8). Therefore, proposed mechanism for the Pb^{2+} induced color transition is revealed in Fig. 1b. As to Pb^{2+} , it should have a maximum coordination number of six. Thus, it is assumed that five ether oxygens in 5EG group and one carboxyl oxygen in PCDA are the six sites in PDA-1 which involved in Pb^{2+} binding forming an octahedral structure.⁵⁰ The strong complexation behaviour of 5EG and carboxylate to Pb^{2+} could conspire the perturbation of the PDA backbone, which dominated the color change behaviour of strips.

Chromatism dependent on the presence of Pb^{2+} and temperature

Thermochromatism, as an inherent characteristic of PDA, is

strongly coupled to pendent side chain conformation.²⁹ Consequently, we anticipated that the chromatism of strips is not only depend on the concentration of Pb^{2+} , but also relied on temperature. Hereby, in the next phase of the investigation, we explored the thermochromatism of newly synthesized PDA-1 by gradually heating the PDA-1/PAN-6 strips from 25 to $60^\circ C$. As distinctly illustrated in Fig. 2a (top line), the strips showed a two stepped color transition, while the first step appeared at the temperature around $40^\circ C$ (blue to purple) and the second step observed around $60^\circ C$ (purple to red). Evidence for the formation of PDA-1 and the nature of blue-to-red color transition in PDA-1/PAN-6 was probed by using Raman spectroscopy. As shown in Fig. S4, the acetylenic stretching band of DAs occurs at 1557 cm^{-1} . After UV irradiation, the acetylenic stretching band disappears and two bands, associated with conjugated alkyne-alkene structures of blue-phase PDA-1, appear at $2082 (C\equiv C)$ and $1450 (C=C) \text{ cm}^{-1}$, indicating that most of DAs are transformed to PDA-1. The Raman spectrum of the red-phased PDA-1 clearly demonstrates that the alkyne-alkene bands shift to higher frequencies at 2122 and 1517 cm^{-1} , proving the distortion of conjugated yne-ene chain induced by temperature. The corresponding CR% value between each temperature point to $25^\circ C$ is revealed in Fig. 2b, the temperature-dependent color responses show a stable range from 25 to $35^\circ C$ (indicated by red dotted circle) and the highest CR% value occurs at $60^\circ C$. Moreover, the strips did not return to original blue when the temperature cooled to $25^\circ C$, there is no doubt that PDA-1 is an irreversible thermochromic material. In this case, the effect of temperature have to be taken into account. Accordingly, those temperature-dependent strips at each point show in top line of Fig. 2a are set as free samples.

When $4 \mu M Pb^{2+}$ liquor was introduced under different temperature for 30 min, as depicted in Fig. 2a (bottom line), except incubating at 25 and $30^\circ C$, the strips subjected to the

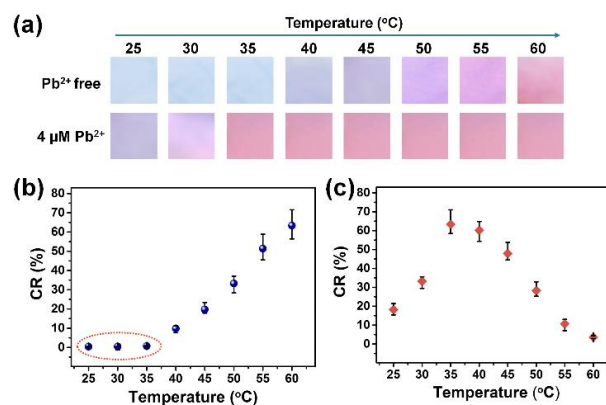


Fig. 2. (a) The corresponding optical images from left to right display the color changes caused by the addition of $0 \mu M$ (top line), and $4 \mu M Pb^{2+}$ (bottom line), upon heating from 25 to $60^\circ C$. (b) The CR% of strips between each temperature point with $25^\circ C$ in the Pb^{2+} free liquor. (c) The CR% of strips between Pb^{2+} free sample and $4 \mu M Pb^{2+}$ detect sample at each temperature point.

temperatures range from 35 to 60°C have changed into red. Subsequently, we used CR% between free and reacted samples to evaluate the chromatism generated by Pb^{2+} and temperature (Fig. 2c). It is noteworthy that the CR% at 35°C was a lot larger than that at other ones, indicating the apparently critical role of temperature. Although raising the temperature may enhance the migration of analytes into the strips and result in a stronger localized stimulation, it could lead to even larger color change at the same time. It was found that the CR% of the strips would reach a saturation value (=63), when keeping the concentration of Pb^{2+} stable and elevating the temperature, the thermochromatic behavior would be the dominant factor which cover up the contribution of Pb^{2+} to the strips' chromatic of the above discussion, it could be concluded that 35°C is the optimum temperature for this assay.

The kinetic investigation of the assaying

In order to investigate the blue-to-red transition upon react time, the plots of the absorption at 645 and 550 nm as a function of time following exposure PDA-1/PAN-6 strips to a 4 μM Pb^{2+} liquor at 35°C displayed in Fig. 3a. The observed results is related to a three-step transformation during the assaying: in the initial stages ($t < 25$ min), the absorption at 550 nm simultaneously increased, so as the absorption at 645 nm showed a gradual decrement. When further prolonging the reaction time, a significant color change occurs within 25 min. Apart from that, the absorption of 550 and 645 nm reached a maximum after 30 min. Even kept increasing the time to 60 min, there was still no obvious change at absorbance peak of 550 and 645 nm. Moreover, the corresponding time dependent optical images are shown in Fig. 3b, which were in line with the phenomenon of absorption change. Under this circumstance, for the sake of the accuracy and comparability of assaying result, the react time should be precisely manipulated.

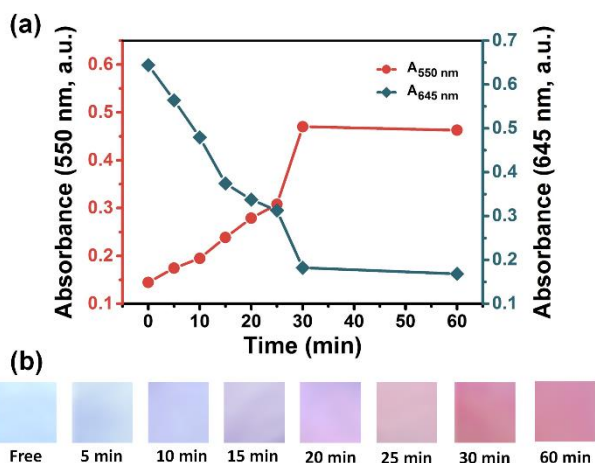


Fig. 3. (a) The plots of the absorption at 645 and 550 nm as a function of time, and (b) the corresponding optical images of the colorimetric strips having been exposure to a 4 μM Pb^{2+} liquor.

Morphology and sensing behaviours of PDA-1 embedded PAN NFM

Despite the PDA-1/PAN-6 strip could trigger a more obvious color change under aforementioned optimal incubation condition, it should be noted that structure features of NFM which may also affect the sensing performance are worthy of detailed exploration. Therefore, we recruited a series of PDA-1 embedded PAN NFM to investigate that. As seen in the Fig. 4a, the sample of PDA-1/PAN-4 exhibited a bead-on-string structure, which contained thin fibers (diameter of 107 ± 29 nm) with a high density of bead defects (average size is 1.64 μm) along the fiber axis. The formation of this morphology could be attributed to the low viscosity polymer solutions.⁵¹ In the case of PDA-1/PAN-6 strip, the morphology of the nanofibers was greatly changed. As shown in the Fig. 4b, the nanofibers exhibit well-defined fibrous morphology with good structural stability. They are continuous, uniform, and have a diameter of 152 ± 25 nm. Hence the increasing PAN contents not only increased the diameter of fibers but also showed bead-free structure, which was also demonstrated by PDA-1/PAN-8 sample. As to the FE-SEM image of PDA-1/PAN-8 displayed in Fig. 4c, it possessed a well-distributed nanofibrous structure, the diameter of nanofibers (234 ± 50 nm) is about 2 times larger than the PDA-1/PAN-4 one. Moreover, the shelf time of white and blue-phase nanofibers is longer than previously published reports (Fig. S5),²⁷ they could show no apparent color change at least 6 month.

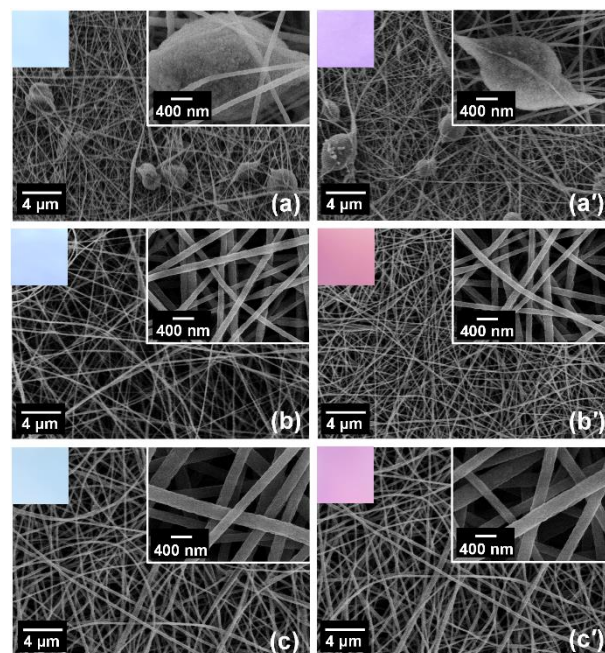


Fig. 4. FE-SEM images of free samples consisted with (a) PDA-1/PAN-4, (b) PDA-1/PAN-6, and (c) PDA-1/PAN-8. (a'), (b'), and (c') are the corresponding samples after incubated in the HEPE buffer spiked with 4 μM Pb^{2+} . Insets show the corresponding optical images.

Distinctive blue color of all free samples are observed inset in Fig. 4a-c, confirming the polymer chain backbone were retained during the electrospinning. By exposure the above-mentioned three kinds of strips to $4 \mu\text{M}$ Pb^{2+} liquor for 30 min, interestingly, as presented inset Fig. 4a'-c', the PDA-1/PAN-8 possesses a CR of 30.4 (blue to amaranth) which is higher than PDA-1/PAN-4 (blue to purple, $\text{CR}\%=23.3$), and the PDA-1/PAN-6 strip has exhibited the largest color transformation (blue to red, $\text{CR}\%=61$). Besides, the sensing behaviour of casting film was explored here. As shown in Fig. S6, due to the limited SSA and poor wettability,^{44, 52} the casting film consisted of leaf-like aggregates displayed a constant blue color ($\text{CR}\% \approx 0$) after Pb^{2+} assaying, which is effective proving the capacity of nanofibrous matrix to enhance the sensitivity.

Quantitatively analysis of porous structure

In consideration of previous reports on NFM based sensors, SSA is the key concern for sensitivity.^{53, 54} As shown in Fig. 3a,

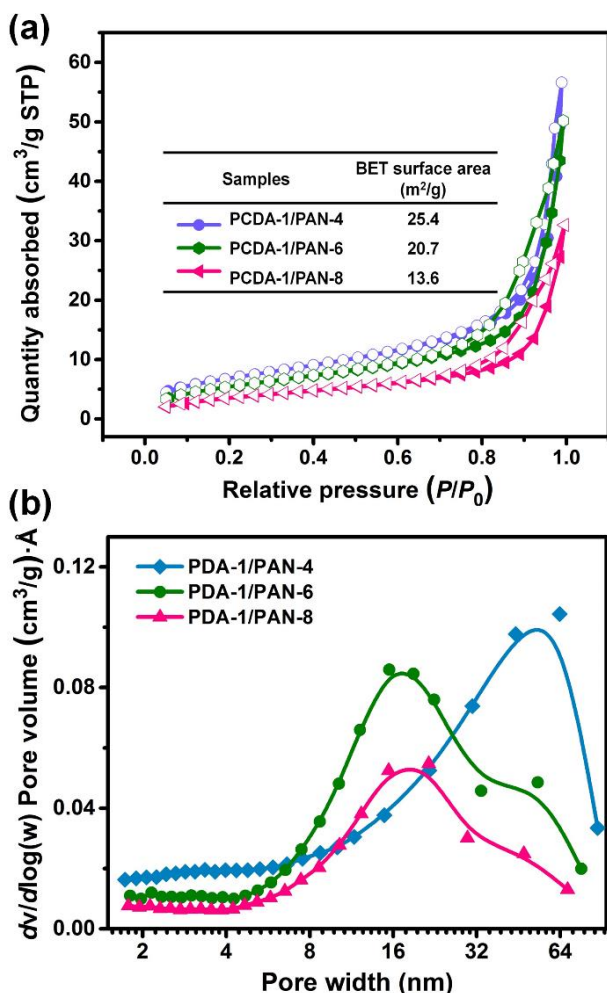


Fig. 5. (a) N_2 adsorption-desorption isotherms of relevant PDA-1/PAN-4, PDA-1/PAN-6, and PDA-1/PAN-8 strips. (b) Pore distribution of relevant strips using the BJH method.

all curves exhibited the isotherm of type IV according to the IUPAC classification.⁵⁵ A series of typical adsorption behaviours including monolayer adsorption, multilayer adsorption and capillary condensation could be observed, revealing characteristics of mesopores within the as prepared membranes.⁵⁶ And the narrow H1 hysteresis loop during the high pressure region indicated that the mesopores are open, thus, there is no significant interruption between the capillary evaporation and condensation for N_2 .⁵⁷ The relevant BET surface area of PDA-1/PAN strips displayed in the inset of Fig. 5a. It can be found that the SSA of PDA-1/PAN-4 showed a highest value of $25.4 \text{ m}^2/\text{g}$, whereas the PDA-1/PAN-6 and PDA-1/PAN-8 showed the SSA of 20.7 and $13.6 \text{ m}^2/\text{g}$, respectively. It is worth noting that a certain decrease of the surface area due to the increasing the diameter of PAN. Theoretically, the strips with a large SSA should result in larger $\text{CR}\%$, however, an unusual phenomenon is observed here, the PDA-1/PAN-4 with the highest SSA showed a minimum $\text{CR}\%$ on the contrary. That is because during the electrospinning, the majority self-assembly of DAs would rather takes place in the bead defect structure than along the fibers, yielding PDA-1 microbeads with 1D arrangement.⁵⁸ Under this circumstance, the effective SSA is significantly shrink attributed to the bead-on-string structure, so as the performance.

The fascinate adsorption isotherms of as-prepared PDA-1/

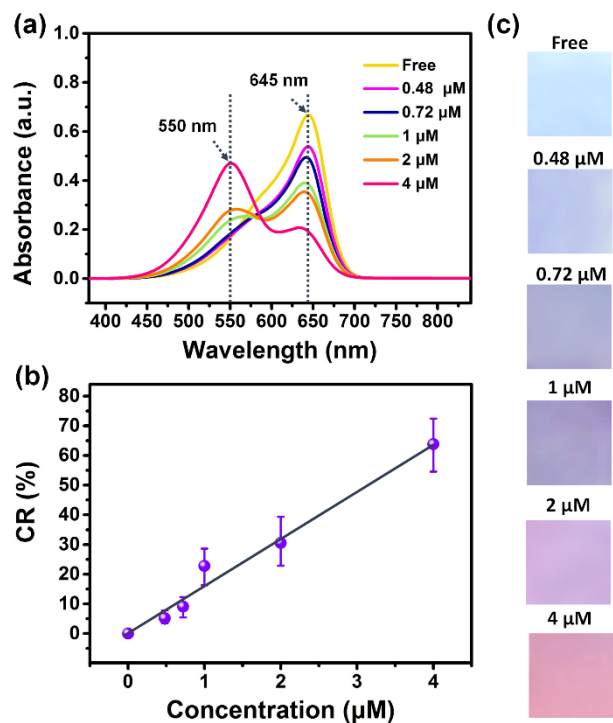


Fig. 6. (a) UV-vis absorbance spectra, (b) CR %, and (c) optical images of strips after incubated with HEPES buffer spiked with increasing concentration of Pb^{2+} for 30min at 35°C .

PAN strips enabled us to deeply investigate their porous structure. Herein, quantitatively pore size distribution (PSD) analysis was achieved by employing the Barrett–Joyner–Halenda (BJH) method.⁵⁹ The representative BJH PSD curves over the range of 2–80 nm shown in Fig. 3b reveal a typically polydisperse porous structure and a primary PSD in the range 10–60 nm, and well-developed peaks centred at 20 nm could be observed in PDA-1/PAN-6 and PDA-1/PAN-8 samples, indicating the mesoporous structure which provided numerous microporous channels that could significantly boost the Pb^{2+} adsorption^{51, 60}, which is beneficial for enhancing the sensing performance. Moreover, it could be observed that the peak value of PDA-1/PAN-4 shift to 54 nm (microsporous structure), which was in constant with the above CR% result.

Analytical performance of strips

We next focused our attention on evaluating the possibility that color change could be promoted by the ligand-receptor reaction between Pb^{2+} and strips. To investigate this proposal, a set of PDA-1/PAN-6 strips, were exposed to independent Pb^{2+} liquors

with varied concentrations at 35°C for 30 min. The UV-vis spectra of each sample were recorded to monitor the progress of blue-to-red transition upon the addition of Pb^{2+} (Fig. 6a). As we anticipated, upon introducing Pb^{2+} liquors, a decrease of absorption at 645 nm, with a simultaneous increase of absorption at 550 nm, indicating the strips demonstrate a typical blue-to-red transition. Furthermore, the CR% versus the Pb^{2+} concentration were plotted in Fig. 6b, where it could be seen that, a good linear correlation between the CR and the Pb^{2+} in a concentration range 0.48 to 4 μM were obtained. The linear response could be represented by the equation: $y = 0.47x + 15.99$, with $R^2 = 0.97$. Based on this correlation curve, therefore, a quantitative analysis of an unknown Pb^{2+} concentration is also achievable. The digital images depicted in the Fig. 6c undergoes an instant blue-to-red color change upon exposure to Pb^{2+} , significantly, it was found that even the addition of trace Pb^{2+} (0.48 μM) could lead a visible color change (CR% = 5.1), which is much lower than that of Narkwiboonwong's work (5 μM).⁴⁹ While this detection limit is imposed by our naked eye, and could be much better under the assistance of equipment.

Psychophysical and neurobiological studies indicate that the human visual system have limited resolving capability at identifying color changes. Therefore, to extract color information and simplify manipulation, chromatic aberration quantization needs to be implemented. Firstly, the UV-vis

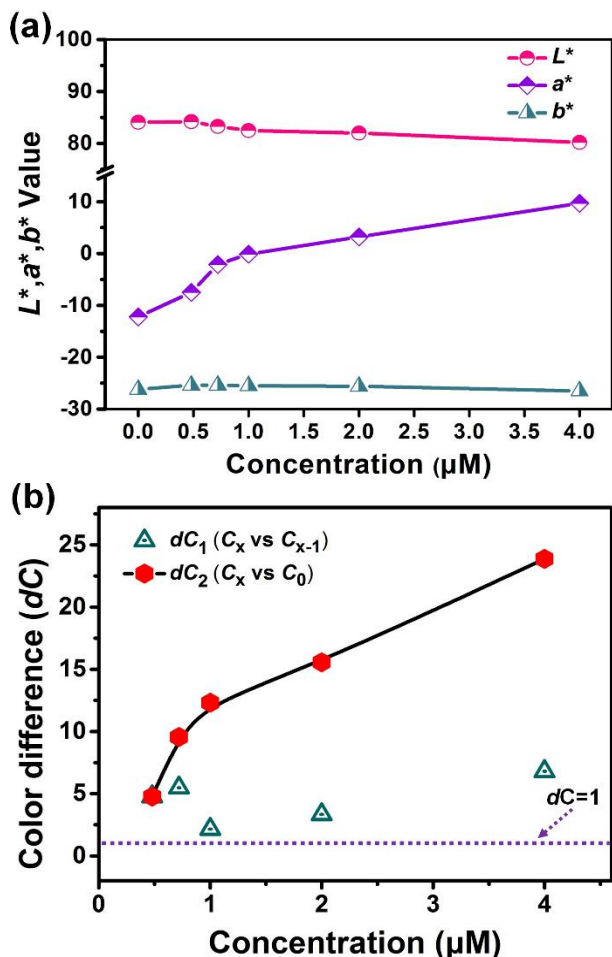


Fig. 7. (a) (L^* , a^* , and b^*) color values calculated from the measured absorption spectra as a function of the concentration of Pb^{2+} . (b) Quantitative sensitivity d_e (S_0 vs. S_x) and gradient color difference d_e (S_x vs. S_{x+1}) values as a function of the concentration of Pb^{2+} .

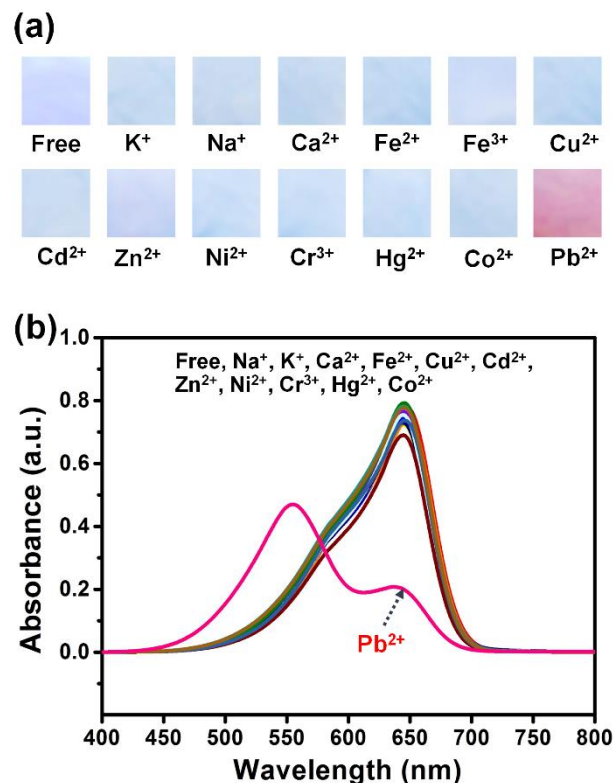


Fig. 8. (a) Optical images, and (b) UV-vis absorbance spectra of strips after incubated in HEPES buffer spiked with 4 μM Pb^{2+} and 10 μM various other metal ions for 30 min at 35°C.

spectrum were converted into the CIE *Lab* color space by applying a converting method. Fig. 7a reveals the converted L^* (lightness), a^* (redness), b^* (yellowness) values as a function of the concentration of Pb^{2+} .⁴⁴ The initial three values of L^* , a^* , b^* values corresponding to free sample are 84.1, -12.2, -26.2, respectively, which is consistent with the blue color of free one. Upon continuously increasing the concentration, a region with stable b^* values and slight rise of a^* value related to the vivid color change from blue to red which not only had a good agreement with the optical images shown in Fig. 6c, but also fit the decreasing rate of L^* parameter. Subsequently, the chromatic aberration between two samples (s_1 , s_2) were calculated based on Euclidean distance (d_e) equation as: $d_e(s_1, s_2) = [(L^*s_1 - L^*s_2)^2 + (a^*s_1 - a^*s_2)^2 + (b^*s_1 - b^*s_2)^2]^{1/2}$, and when the value of d_e is above 1 LAB unit, that means the chromatic aberration is approximately equal to the threshold of perceptual color change.⁶¹ Herein, we adopted two types of chromatic aberration to appraise the naked eye identification ability: $d_e(s_0, s_x)$ which refer to the chromatic aberration between detecting samples to free samples and $d_e(s_x, s_{x+1})$ which represented the chromatic aberration of two adjacent detecting samples. The calculated values of $d_e(s_0, s_x)$ and $d_e(s_x, s_{x+1})$ versus Pb^{2+} revealed in Fig. 7b, and it is worthy to point out that all the chromatic aberration obtained were higher than 1 CIE LAB unit, there was no doubt that all of them could readily be identified by naked eyes.

Having proved the high sensitivity of the strips, we next investigated the CR towards the metal ions. The strips displayed a selective and clear blue to red transition only with 4 μM Pb^{2+} among various metal cations with a concentration of 10 μM tested, including Na^+ , K^+ , Ca^{2+} , Fe^{2+} , Cu^{2+} , Cd^{2+} , Zn^{2+} , Ni^{2+} , Cr^{3+} , Hg^{2+} , Pb^{2+} , and Co^{2+} (Fig. 8a). The colorimetric behavior of strip after addition of metal ions was also studied by UV-vis spectroscopy. As shown in Fig. 8b, only the Pb^{2+} could lead to a robust spectral change: the absorption intensity at 645 nm decreased and a new absorption band at 550 nm, which ascribed to the red form of PDA-1, emerged. According to the previous studies, PCDA derived PDA should not responsible for the selectivity even it is known to have an ionochromic property,²⁷ we therefore suspected that this discriminating power can be ascribe to the unique characteristics of 5EG chains. As to crown ether derivatives, they can form complexes with Pb^{2+} , which possess a higher complexation constant than those with other metal ions.⁶² Moreover, the ability of selectively extracting metal cations can be improved by derivatizing them with function groups (e.g., carboxylic acids and carboxylic esters).^{63, 64} All above results proved that the strips could act as a selective probe to detect Pb^{2+} in aqueous solutions.

Conclusion

In summary, we have successfully prepared a novel, facile, selective colorimetric strip by embedding PDA into the PAN NFM. Compared with the casting film based one, our strip displayed a much higher sensitivity toward Pb^{2+} and had a

naked eye detection limit of 0.48 μM . The blue-to-red color change signal was maximized by manipulating the optimal molar ratio of bi-component DAs (PCDA/PCDA-5EG = 3/7). Meanwhile, the most suitable incubation time (30 min) and temperature (35°C) were also optimized to achieve a higher color response. Moreover, the morphology, SSA and porous structure of relevant PDA embedded PAN NFM could be regulated by turning the concentration of PAN, which displayed profound influence on sensing performance. Also, the anti-interference ability of the strip was demonstrated in the presence of other metal cations at high concentrations (10 μM). The analysis for quantitative and gradient sensitivity using a novel colorimetric framework related to human perception has confirmed the obvious perceivable color changes over Pb^{2+} . This work provides a convenient, selective and sensitive naked eye Pb^{2+} detection method which has potential application in the in situ and real-time detection in the future.

Acknowledges

This work is supported by the National Basic Research Program of China (973 Program, 2012CB525005), the National Natural Science Foundation of China (No. 51173022, 51273038 and 51322304), the Fok Yingtong Foundation (131070), the Program for New Century Talents of the University in China, the Fundamental Research Funds for the Central Universities, and the "DHU Distinguished Young Professor Program".

Notes and references

^a Key Laboratory of Textile Science & Technology, Ministry of Education, College of Textiles, Donghua University, Shanghai 201620, China. E-mail: binding@dhu.edu.cn

^b Nanomaterials Research Center, Modern Textile Institute, Donghua University, Shanghai 200051, China

^c Department of Occupational and Environmental Health, School of Public Health, Fourth Military Medical University, Xi'an, Shanxi 710032, China. E-mail: jy_chen@fmmu.edu.cn

† Electronic Supplementary Information (ESI) available: The details ¹H and ¹³C NMR spectroscopy for the structural confirmation of PCDA-5EG, the corresponding optical images of PDA embedded strips derived from PCDA and PCDA-5EG before and after exposure to Pb^{2+} , the Raman spectra of PDA-1/PAN-6 strip in different phase, the optical images showing the stability of white and blue-phase nanofibers within 6 months, and the FE-SEM and optical images of casting film based strip before (a) and after (a') incubated with 4 μM Pb^{2+} . See DOI: 10.1039/b000000x/

1 Neal and T. Guilarte, *Mol. Neurobiol.*, 2010, **42**, 151.

2 Y. Finkelstein, M. E. Markowitz and J. F. Rosen, *Brain Res. Rev.*, 1998, **27**, 168.

3 Q. Zhao, X. Rong, H. Ma and G. Tao, *J. Hazard. Mater.*, 2013, **250–251**, 45.

4 T. S. Nawrot and J. A. Staessen, *Circulation*, 2006, **114**, 1347.

5 M. S. Amato, S. Magzamen, P. Imm, J. A. Havlena, H. A. Anderson, M. S. Kanarek and C. F. Moore, *Environ. Res.*, 2013, **126**, 60.

- 6 Y. Wang, S. Gao, X. Zang, J. Li and J. Ma, *Anal. Chim. Acta*, 2012, **716**, 112.
- 7 J. Djedjibegovic, T. Larssen, A. Skrbo, A. Marjanović and M. Sober, *Food Chem.*, 2012, **131**, 469.
- 8 C. B. Swearingen, D. P. Wernette, D. M. Cropek, Y. Lu, J. V. Sweedler and P. W. Bohn, *Anal. Chem.*, 2004, **77**, 442.
- 9 H. N. Kim, W. X. Ren, J. S. Kim and J. Yoon, *Chem. Soc. Rev.*, 2012, **41**, 3210.
- 10 S. Su, W. Wu, J. Gao, J. Lu and C. Fan, *J. Mater. Chem.*, 2012, **22**, 18101.
- 11 N. Kaur and S. Kumar, *Tetrahedron*, 2011, **67**, 9233.
- 12 Q. He, E. W. Miller, A. P. Wong and C. J. Chang, *J. Am. Chem. Soc.*, 2006, **128**, 9316.
- 13 E. Chow, D. B. Hibbert and J. J. Gooding, *Anal. Chim. Acta.*, 2005, **543**, 167.
- 14 N. A. Rakow and K. S. Suslick, *Nature*, 2000, **406**, 710.
- 15 P. Puiu, in *Optical Nano- and Microsystems for Bioanalytics*, eds. W. Fritzsche and J. Popp, Springer Berlin Heidelberg, 2012, vol. 10, ch. 1, pp. 3.
- 16 H. Li, Q. Zhang, Y. Cai, D.-M. Kong and H.-X. Shen, *Biosens. Bioelectron.*, 2012, **34**, 159.
- 17 F. Chai, C. Wang, T. Wang, L. Li and Z. Su, *ACS Appl. Mater. Interfaces*, 2010, **2**, 1466.
- 18 M. Khairy, S. A. El-Safty, M. A. Shenashen and E. A. Elshehy, *Nanoscale*, 2013, **5**, 7920.
- 19 L. Yu and S. L. Hsu, *Macromolecules*, 2011, **45**, 420.
- 20 D. J. Ahn, E.-H. Chae, G. S. Lee, H.-Y. Shim, T.-E. Chang, K.-D. Ahn and J.-M. Kim, *J. Am. Chem. Soc.*, 2003, **125**, 8976.
- 21 A. Potisatityuenyong, R. Rojanathanes, G. Tumcharern and M. Sukwattanasinitt, *Langmuir*, 2008, **24**, 4461.
- 22 D.-H. Park, J. Hong, I. S. Park, C. W. Lee and J.-M. Kim, *Adv. Func. Mater.*, 2014, **24**, 5186.
- 23 R. W. Carpick, D. Y. Sasaki and A. R. Burns, *Langmuir*, 2000, **16**, 1270.
- 24 S.-H. Eo, S. Song, B. Yoon and J.-M. Kim, *Adv. Mater.*, 2008, **20**, 1690.
- 25 J. Lee, H. Jun and J. Kim, *Adv. Mater.*, 2009, **21**, 3674.
- 26 Q. Xu, S. Lee, Y. Cho, M. H. Kim, J. Bouffard and J. Yoon, *J. Am. Chem. Soc.*, 2013, **135**, 17751.
- 27 J. Guo, L. Yang, L. Zhu and D. Chen, *Polymer*, 2013, **54**, 743.
- 28 S. W. Lee, C. D. Kang, D. H. Yang, J. S. Lee, J. M. Kim, D. J. Ahn and S. J. Sim, *Adv. Func. Mater.*, 2007, **17**, 2038.
- 29 X. Chen, G. Zhou, X. Peng and J. Yoon, *Chem. Soc. Rev.*, 2012, **41**, 4610.
- 30 X. Pan, Y. Wang, H. Jiang, G. Zou and Q. Zhang, *J. Mater. Chem.*, 2011, **21**, 3604.
- 31 K. M. Lee, X. Chen, W. Fang, J.-M. Kim and J. Yoon, *Macromol. Rapid. Commun.*, 2011, **32**, 497.
- 32 D. H. Kang, H.-S. Jung, J. Lee, S. Seo, J. Kim, K. Kim and K.-Y. Suh, *Langmuir*, 2012, **28**, 7551.
- 33 A. Kumar, U. J. Erasquin, G. Qin, K. Li and C. Cai, *Chem. Commun.*, 2010, **46**, 5746.
- 34 D. H. Kang, H.-S. Jung, N. Ahn, S. M. Yang, S. Seo, K.-Y. Suh, P.-S. Chang, N. L. Jeon, J. Kim and K. Kim, *ACS Appl. Mater. Interfaces*, 2014, **6**, 10631.
- 35 J. Lee and J. Kim, *Chem. Mater.*, 2012, **24**, 2817.
- 36 X. Wang, X. Sun, P. A. Hu, J. Zhang, L. Wang, W. Feng, S. Lei, B. Yang and W. Cao, *Adv. Func. Mater.*, 2013, **23**, 6044.
- 37 J. Lee, H. T. Chang, H. An, S. Ahn, J. Shim and J.-M. Kim, *Nat. Commun.*, 2013, **4**, 2461.
- 38 H. Jiang, Y. Wang, Q. Ye, G. Zou, W. Su and Q. Zhang, *Sensor. Actuat. B-Chem.*, 2010, **143**, 789.
- 39 J. Yoon, S. K. Chae and J.-M. Kim, *J. Am. Chem. Soc.*, 2007, **129**, 3038.
- 40 S. Lee, Y. Cho, B. U. Ye, J. M. Baik, M. H. Kim and J. Yoon, *Chem. Commun.*, 2014, DOI: 10.1039/C4CC03511A.
- 41 M.-C. Lim, Y.-J. Shin, T.-J. Jeon, H.-Y. Kim and Y.-R. Kim, *Anal. Bioanal. Chem.*, 2011, **400**, 777.
- 42 B. Ding, M. Wang, X. Wang, J. Yu and G. Sun, *Mater. Today*, 2010, **13**, 16.
- 43 B. Ding, Y. Si, X. Wang, J. Yu, L. Feng and G. Sun, *J. Mater. Chem.*, 2011, **21**, 13345.
- 44 Y. Li, Y. Si, X. Wang, B. Ding, G. Sun, G. Zheng, W. Luo and J. Yu, *Biosensor. Bioelectron.*, 2013, **48**, 244.
- 45 K. S. Jeon, R. Nirmala, R. Navamathavan and H. Y. Kim, *Ceram. Int.*, 2013, **39**, 8199.
- 46 B. W. Davis, A. J. Burris, N. Niammont, C. D. Hare, C.-Y. Chen, M. Sukwattanasinitt and Q. Cheng, *Langmuir*, 2014, **30**, 9616.
- 47 H. Li, Q. Zheng and C. Han, *Analyst*, 2010, **135**, 1360.
- 48 R. Frech and W. Huang, *Macromolecules*, 1995, **28**, 1246.
- 49 P. Narkwiboonwong, G. Tumcharern, A. Potisatityuenyong, S. Wacharasindhu, M. Sukwattanasinitt, *Talanta*, 2010, **83**, 872.
- 50 F. Zhao, E. Repo, D. Yin and M. E. T. Sillanpää, *J. Colloid. Interf. Sci.*, 2013, **409**, 174.
- 51 M. W. Lee, S. An, S. S. Latthe, C. Lee, S. Hong and S. S. Yoon, *ACS Appl. Mater. Interfaces*, 2013, **5**, 10597.
- 52 X. Wang, J. Wang, Y. Si, B. Ding, J. Yu, G. Sun, W. Luo and G. Zheng, *Nanoscale*, 2012, **4**, 7585.
- 53 B. Ding, M. Wang, J. Yu and G. Sun, *Sensors*, 2009, **9**, 1609.
- 54 M. K. Tiwari, A. L. Yarin and C. M. Megaridis, *J. Appl. Phys.*, 2008, **103**, 10.
- 55 Y. Si, T. Ren, B. Ding, J. Yu and G. Sun, *J. Mater. Chem.*, 2012, **22**, 4619.
- 56 B. Li, B. Jiang, D. J. Fauth, M. L. Gray, H. W. Pennline and G. A. Richards, *Chem. Commun.*, 2011, **47**, 1719.
- 57 Y. Duan, D. R. Luebke, H. W. Pennline, B. Li, M. J. Janik and J. W. Halley, *J. Phys. Chem. C*, 2012, **116**, 14461.
- 58 S. K. Chae, H. Park, J. Yoon, C. H. Lee, D. J. Ahn and J. M. Kim, *Adv. Mater.*, 2007, **19**, 521.
- 59 B. Ding, J. Lin, X. Wang, J. Yu, J. Yang and Y. Cai, *Soft Matter*, 2011, **7**, 8376.
- 60 H. Wang, P. Zhang, X. Ma, S. Jiang, Y. Huang, L. Zhai and S. Jiang, *J. Hazard. Mater.*, 2014, **265**, 158.
- 61 M. M. Hawkeye and M. J. Brett, *Adv. Fun. Mater.*, 2011, **21**, 3652.
- 62 W. S. Xia, R. H. Schmehl, C. J. Li, J. T. Mague, C. P. Luo and D. M. Guldi, *J. Phys. Chem. B*, 2002, **106**, 833.
- 63 H. Y. An, J. S. Bradshaw, R. M. Izatt and Z. M. Yan, *Chem. Rev.*, 1994, **94**, 939.
- 64 W. Walkowiak, W. A. Charewicz, S. I. Kang, I. W. Yang, M. J. Puglia and R. A. Bartsch, *Anal. Chem.*, 1990, **62**, 2018.